Annals of Glaciology 20 1994

Characteristics of bubble volumes in firn–ice transition layers of ice cores from polar ice sheets

TAKAO KAMEDA
Kitami Institute of Technology, Koencho 165, Kitami, Hokkaido 090, Japan

RENJI NARUSE
Institute of Low Temperature Science, Hokkaido University, Sapporo, Hokkaido 060, Japan

ABSTRACT. The air-bubble formation process has been studied experimentally by using five ice cores from the Greenland and Antarctic ice sheets. Bubble volumes in firn–ice samples were measured by a classical method based on Boyle Mariotte's law for an ideal gas. It was found that the bubble volume varies with depth as a function of bulk density in the firn–ice transition layer, which is represented by an exponential function of firn density. Air bubbles start to form rapidly at a bulk density of 0.763–0.797 Mg m^{-3}. This density (ρ_{ib}) seems to be correlated with the ice temperature in the ice sheets; ρ_{ib} increases with a decrease in the ice temperature. V_b shows the maximum value in the density range 0.819–0.832 Mg m^{-3}. The corresponding porosity of the density ranges between 0.110 and 0.097. This porosity does not seem to correlate with ice temperature or accumulation rate at the coring site. These characteristics of firn densities probably affect the amount of entrapped air in glacier ice (total air content) in polar ice sheets.

1. INTRODUCTION

Air bubbles in polar glacier ice are formed during the densification process of firn to ice. Air channels in firn become isolated and form air bubbles during the process. This process has been studied by measuring air permeability of firn ice samples (Maeno and others, 1978; Langway and others, 1993) and by measuring total bubble volume in firn–ice samples (Schwander and Stauffer, 1984; Stauffer and others, 1985; Martinerie and others, 1992; Schwander and others, 1993). Schwander and Stauffer (1984) found that this process occurred rapidly from 64 to 76 m depth in an ice core from Siple Station, Antarctica. The bubble-formation process at Summit in Greenland was examined by Martinerie and others (1992) and by Schwander and others (1993). However, air-bubble formation processes by bubble-volume measurements have not been examined in detail, except for these two ice cores.

We focus on total bubble volumes in firn–ice transition layers using five ice cores from the Greenland and Antarctic ice sheets and discuss the regional characteristics of the bubble-volume profile. The method of volume measurement is briefly described.

2. METHODS OF MEASUREMENTS

For measurements of density and total bubble volumes, we cut cylindrical samples 35–40 mm in diameter and 40–60 mm in length. Total bubble volume, defined as the total volume of pores that are sealed by the ice matrix, was measured by a method similar to that developed by Schwander and Stauffer (1984). They employed a classical method based on Boyle–Mariotte's law for an ideal gas (pressure × volume = constant at a constant temperature). We modified the method as follows: the ice sample was disconnected from the measuring system when air pressures in the system were measured. This modification enabled us to eliminate the effect of vapor pressure of ice during the measurements of pressure drops (ΔP_1 and ΔP_2 in the following paragraph).

Figure 1 shows a schematic diagram of our measuring system. For the measurements, volume V_1 containing a firn ice sample is disconnected from the atmosphere and connected to $V_2 + V_3$ that was evacuated previously (ΔP_1; about 30 Torr). Opening valve 1, air in the V_1 (atmospheric pressure, P_a) is expanded to V_2 and V_3. After 30 s, valve 1 is closed and the pressure drop ΔP_2 in V_2 and V_3 is measured. Assuming an isothermal process, the impermeable volume of the sample ($V_i + V_t$) is measured using the following equation:

$$P_a\{V_1 - [V_i + V_t]\} + [P_a - \Delta P_1][V_2 + V_3] = [P_a - \Delta P_2]\{V_1 - [V_i t + V_t] + V_2 + V_3\} \quad (1)$$

where P_a is atmospheric pressure; ΔP_1 is first pressure drop in V_2 by a hand pump; ΔP_2 is second pressure drop in $V_1 + V_2 + V_3$ by an expansion of air; V_1 is the inner volume of V_1 (169.46 cm^3); V_2 is the inner volume of V_2 (82.52 cm^3); V_3 is the inner volume of tubes in the measuring system (30.58 cm^3); V_i is volume of the ice

https://doi.org/10.3189/1994AoG20-1-95-100 Published online by Cambridge University Press

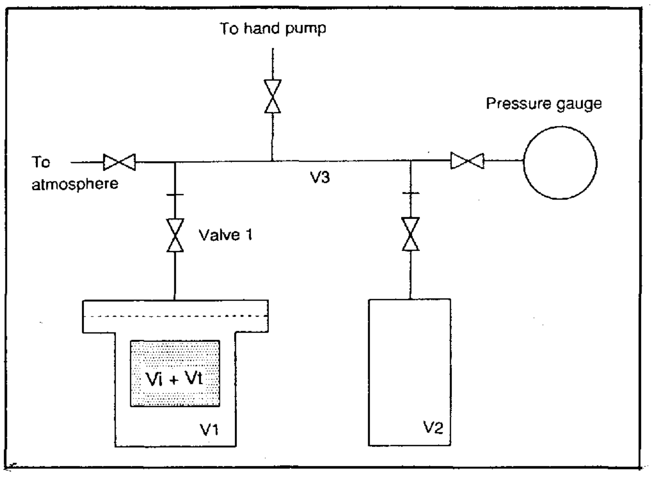

Fig. 1. Schematic diagram of a system for measurement of bubble volumes in firn–ice samples.

matrix and V_t is total bubble volume in a firn–ice sample. V_i is obtained from measurements of weight and temperature of firn–ice samples using a bubble-free ice density (Bader, 1964). The weights of samples were measured with an absolute accuracy of ± 0.01 g and temperature was measured with an accuracy of ± 0.1°C. The pressure drops (ΔP_1 and ΔP_2) were measured with an accuracy of ± 0.04 Torr (type PH-22-D, SOKKEN Co. Ltd). Then V_t is calculated from Equation (1).

Bubble volume (V_b) is defined as the total bubble volume (V_t) per weight of the sample ($V_b = V_t/m$; m is the weight of the sample). Air-channel volume (V_a) is defined as the total air-channel volume per weight of the sample. Air channels refer to pores which connect with surfaces of the samples. As total pore volume per unit mass of the sample is identical with $V_a + V_b$, V_a is calculated as follows:

$$V_a = 1/\rho - 1/\rho_i - V_b \qquad (2)$$

where ρ is the bulk density of the sample and ρ_i is the bubble-free ice density at t°C (Bader, 1964).

Errors in the volume measurements were investigated using bubble-free single crystals of ice taken from Mendenhall Glacier, Alaska (Higashi, 1988). It was found that the standard deviation of the volume measurements of the ice samples was 0.11 cm^3. Relations between sample volumes and analytical errors per unit mass (ΔV) are shown in Figure 2. Standard deviations per unit mass of ice are expressed by two curves. For 30–70 g ice samples, the errors in the measurements were in the range ± 0.004 to ± 0.002 cm^3 g^{-1}, i.e. ± 0.004 to $\pm$ 0.002 m^3 Mg^{-1}.

Optical microscopic observation was conducted on thin-section samples from each ice core to investigate the air-bubble size, shape and configuration.

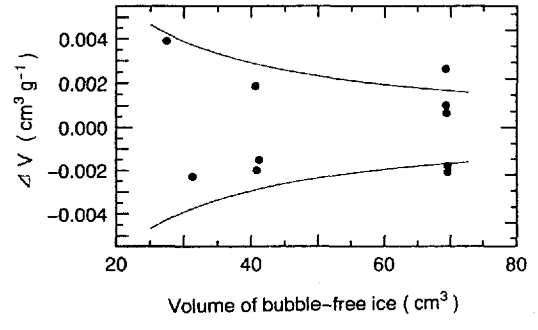

Fig. 2. The accuracy of bubble-volume measurements for bubble-free ice samples with standard-deviation lines.

3. RESULTS

The positions, ice temperatures and annual accumulation rates of five ice-coring sites are summarized in Table 1. Results of bubble volumes (V_b) and air-channel volumes (V_a) of these ice cores are shown in Figure 3. It should be noticed that air bubbles are rapidly formed at the following depth intervals: H231 (from about 41–49 m depth); Mizuho (about 44–53 m depth); G15 (about 63 74 m depth); AC (about 72–80 m depth) and site J (about

Table 1. Glaciological data and references for Antarctic and Greenland ice cores. T_c was measured at the following depths in the firn–ice transition layer: H231 (40 m), Mizuho Station (51 m), G15 (68 m), AC (80 m) and site J (60 m)

Site name	*Location*		*Ice temperature*	*Accumulation rate*	*References for T and A data*
	lat.	long.	°C	m w.e. year^{-1}	
Antarctica					
H231	69°46′ S	42°27′ E	25.4	0.11	Suzuki and Shiraishi (1982); Takahashi and others (1994)
Mizuho Station	70°42′ S	44°22′ E	–34.28	0.09	Fujii (1978); Nakawo and others (1989)
G15	71°11′ S	45°58′ E	37.8	0.10	Moore and others (1991); personal communication from H. Narita
AC	74°12′ S	34°59′ E	–43.8	0.06	Satake and others (1986); personal communication from Y. Ageta
Greenland					
Site J	66°52′ N	46°16′ W	–16.7	0.39	Shoji and others (1991)

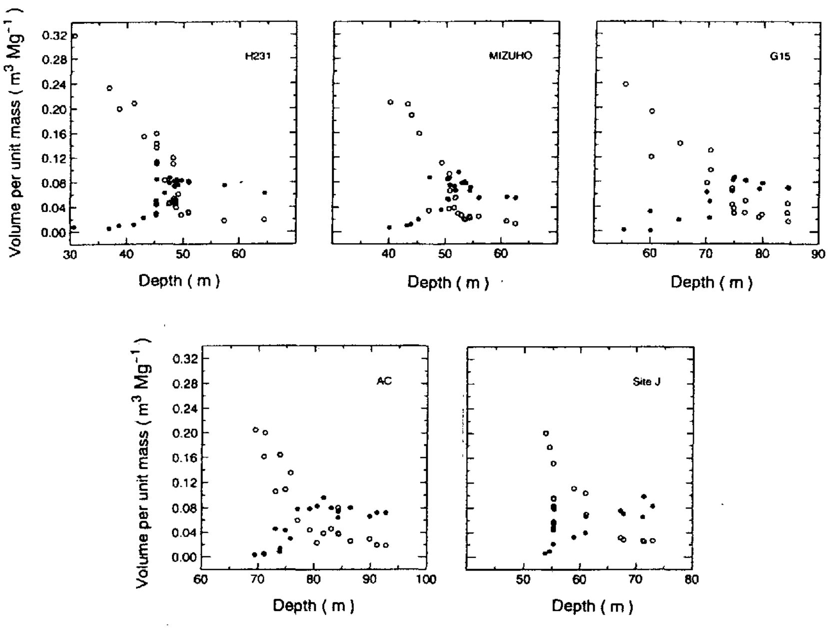

Fig. 3. Bubble volume and air-channel volumes versus depth in five ice cores from the Greenland and Antarctic ice sheets.

54–65 m depth). Air-channel volumes rapidly decrease in these depth intervals. These characteristic features of bubble formation are confirmed by microscopic observations on thin-section samples from each core.

4. DISCUSSION

An examination was made to find a relation between bulk density (ρ) and bubble volume (V_b) using the bubble-volume data in Figure 3. It was found that there is a linear relation between ρ and $\ln(V_b)$, as shown in Figure 4, in a density range from 0.75 to 0.825 Mg m^{-3}. The straight line for the lower density of 0.825 Mg m^{-3} in Figure 4 is expressed as follows:

$$\ln(V_b) = 48.466\rho - 42.38. \tag{3}$$

Bubble volume (V_b) and density (ρ) are expressed in units of m^3 Mg^{-1} and Mg m^{-3}, respectively. The correlation coefficient and the degrees of freedom of this relation are 0.91 and 68, respectively.

On the other hand, bubble volumes of ice samples at the higher density of 0.825 Mg m^{-3} decrease with bulk density as in the following equation, because the increase in ice density is caused by a decrease of total bubble volume:

$$\begin{aligned} V_b &= \frac{\rho_c}{\rho_i - \rho_c}\frac{\rho_i - \rho}{\rho} V_c \\ &= [\rho_c\rho_i V_c/(\rho_i - \rho_c)][1/\rho - 1/\rho_i] \end{aligned} \tag{4}$$

where ρ_c is a pore close-off density, at which firn turns into ice by the definition of ice, and V_c is bubble volume per unit mass of ice at pore close-off.

We can determine the coefficient in Equation (4) using bubble-volume data, in which densities are over 0.825 Mg m^{-3} and also the average ice temperatures at five sites (−31.19°C) are as follows:

$$V_b = 0.7234\,[1/\rho - 1/\rho_i] \tag{5}$$

where the correlation coefficient and the degrees of freedom are 0.62 and 33, respectively.

Bubble volumes in five ice cores with the calculated curves of Equations (3) and (5) are shown in Figure 5. They show a sharp increase from bulk density of about 0.78 Mg m^{-3} and have a peak value in bulk density between 0.820 and 0.830 Mg m^{-3}. Bubble-volume profiles, expressed by the two curves, have the maximum value (0.091 m^3 Mg^{-1}) at a bulk density of 0.825 Mg m^{-3}.

Results of microscopic observation show that the number and mean diameter of the air bubbles depend on the mean annual temperatures at the coring site: the number of air bubbles per unit mass decreases with temperature and the mean diameter of air bubbles increases with temperature. However, these two factors contribute to an increase in the bubble volume in an opposite way and may cause the data scatter shown in Figure 5.

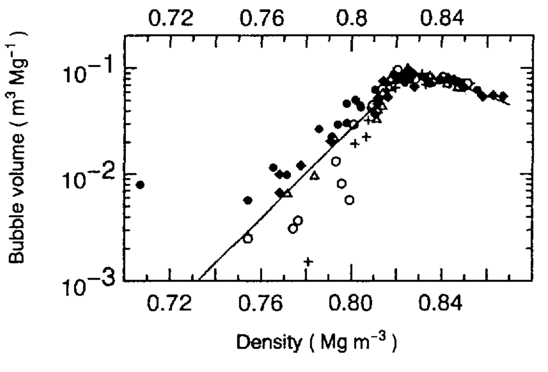

Fig. 4. Relation between logarithm of bubble volume ($\ln(V_b)$) and bulk density (ρ) for five ice cores with calculated fit lines.

https://doi.org/10.3189/1994AoG20-1-95-100 Published online by Cambridge University Press

Table 2. Values of ρ_{cb}, porosity s_{cb}, depth from surface h_{cb}, overburden pressure P_{cb} and corresponding bubble volume V_{cb} for five ice cores

Site name	ρ_{cb} Mg m^{-3}	s_{cb}	*Depth* m	P_{cb} MPa	V_{cb} m^3 Mg^{-1}
H231	0.819	0.110	47	0.29	0.089
Mizuho Station	0.832	0.097	53	0.36	0.089
G15	0.817	0.114	74	0.48	0.098
AC	0.821	0.110	80	0.52	0.094
Site J	0.825	0.102	65	0.42	0.092
Average ± S.D.	0.823±0.005	0.107±0.006	64±12	0.41±0.08	0.092±0.003

In Figure 5, it seems that V_b of H231 and Mizuho are slightly higher than those of other cores in a density range 0.76–0.81 Mg m^{-3}. In order to examine these regional differences of bubble volumes with bulk density, the above methods of two-curve fittings were again employed for each set of coring-site data.

V_b with calculated two-fit curves for each site are shown in Figure 6. The peak bubble volume probably corresponds to completion of the bubble-formation zone in the firn–ice transition layer. This bubble volume is denoted as V_{cb}. Firn density at V_{cb} (ρ_{cb}), porosity ($s_{cb} = 1 - \rho_{cb}/\rho_i$), overburden pressure ($P_{cb}$) and V_{cb} are summarized in Table 2. It was found that ρ_{cb} was in a density range 0.819–0.832 Mg m^{-3}. The standard deviation of ρ_{cb} is 0.005 Mg m^{-3}. This deviation is almost the same as errors in density measurements (= 0.004 Mg m^{-3}).

For examining rapid bubble formation in the firn–ice transition zone, a 10% value of peak bubble volume is selected here as a reference parameter. This bubble volume seems to correspond to the initiation of the rapid bubble-formation zone in the firn–ice transition layer. This bubble volume is denoted as V_{ib}. Firn density at V_{ib} (ρ_{ib}), porosity (s_{ib}), overburden pressure (P_{ib}) and V_{ib} are summarized in Table 3. It was found that ρ_{ib} ranges from 0.763 to 0.797 Mg m^{-3}. The standard deviation of ρ_{ib} is 0.013 Mg m^{-3}. The deviation is about three times larger than the error in the density measurements.

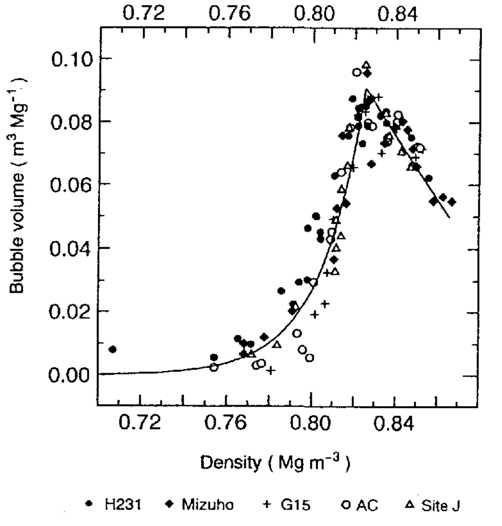

Fig. 5. Relation between air-bubble volume (V_b) and bulk density (ρ) for five ice cores with calculated-fit curves.

The ρ_{ib} and ρ_{cb} with ice temperatures are shown in Figure 7. It seems that ρ_{ib} of four Antarctic ice cores has a correlation with ice temperature (correlation coefficient: $r = 0.81$). The value of ρ_{ib} at site J (0.780 Mg m^{-3}) was slightly larger than the expected value from four Antarctic ice cores. ρ_{cb} does not seem to be correlated with ice temperature or accumulation rate of the coring site.

Table 3. Values of ρ_{ib}, porosity s_{ib}, depth from surface h_{ib}, overburden pressure P_{ib} and V_{ib} (10% of V_{cb}) for five ice cores

Site name	ρ_{ib} Mg m^{-3}	s_{ib}	*Depth* m	P_{ib} MPa	V_{ib} m^3 Mg^{-1}
H231	0.763	0.171	41	0.25	0.009
Mizuho Station	0.768	0.165	44	0.28	0.009
G15	0.797	0.134	63	0.39	0.010
AC	0.791	0.140	72	0.46	0.009
Site J	0.780	0.152	54	0.34	0.009
Average ± S.D.	0.780±0.013	0.152±0.014	55±12	0.34±0.08	0.009±0.000

https://doi.org/10.3189/1994AoG20-1-95-100 Published online by Cambridge University Press

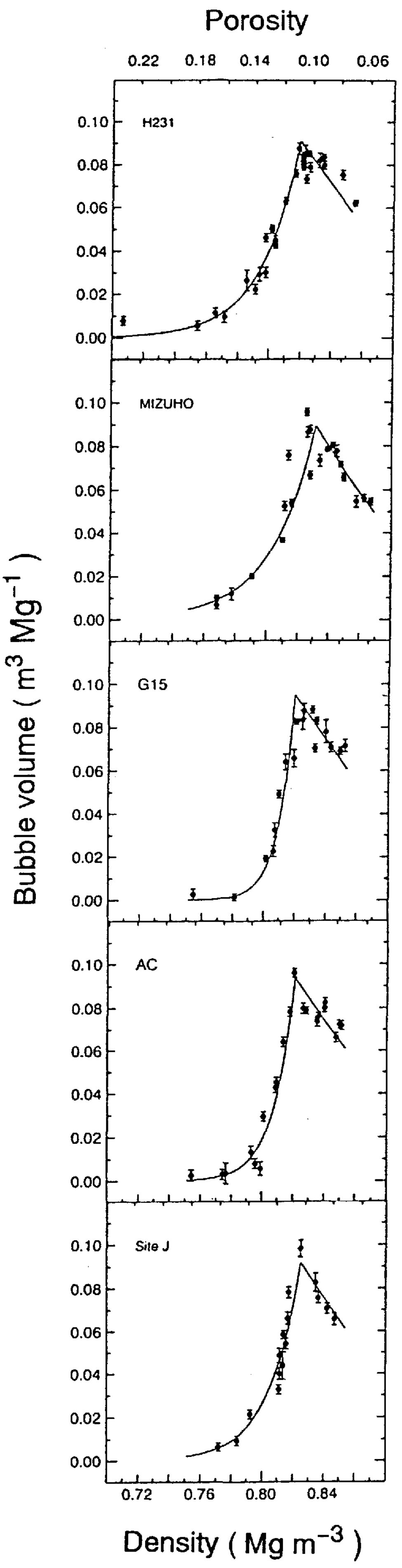

Fig. 6. Relation between bubble volume (V_b) and bulk density (ρ) for each ice core with calculated fit curves.

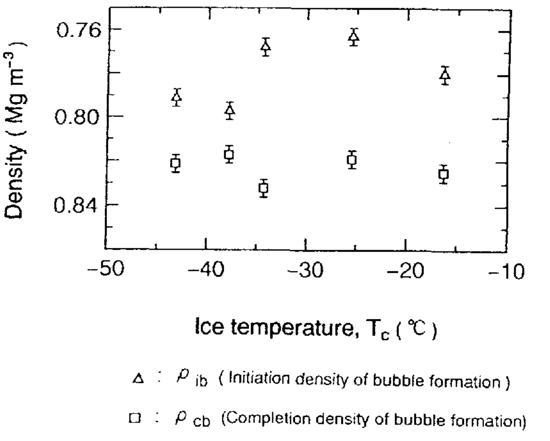

Fig. 7. Relation between ice temperature and ρ_{ib} (triangles) and also ice temperature and ρ_{cb} (squares). ρ_{cb} is identical with peak bubble-volume density.

Overburden pressures for ρ_{ib} and ρ_{cb} (denoted as P_{ib} and P_{cb}, respectively) in ice sheets and ice temperatures are examined in Figure 8. It was found that P_{ib} ranges from 0.25 to 0.46 MPa and P_{cb} ranges from 0.29 to 0.52 MPa. A correlated relation between P_{ib} and ice temperature for four Antarctic ice cores is again observed ($r = 0.93$). A correlated relation between P_{cb} and ice temperature ($r = 0.92$) is also observed.

Kameda and others (1994) have demonstrated that firn-density profiles in ice sheets are determined primarily by overburden pressure and firn temperature contributes to a lesser degree. Thus, density ranges from ρ_{ib} to ρ_{cb} in ice sheets are primarily determined by these two parameters.

5. CONCLUSION

We have measured bubble volumes (V_b) in the firn–ice transition layer using five ice cores from Greenland and Antarctica. It was found that V_b ($m^3\,Mg^{-1}$) in five ice

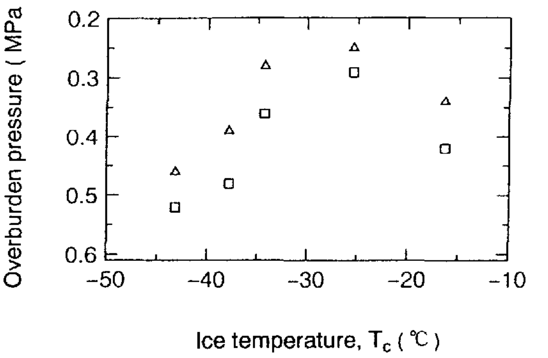

Fig. 8. Relation between ice temperature and P_{ib} (triangles) and also ice temperature and P_{cb} (squares). P_{ib} is identical with the overburden pressure, from which bubble volumes start to increase rapidly. P_{cb} is identical with the overburden pressure at which bubble volume shows the maximum value by two-fit curves.

https://doi.org/10.3189/1994AoG20-1-95-100 Published online by Cambridge University Press

cores was expressed by a function of density as in the following equations:

$$\ln V_b = 48.466\rho - 42.38, \qquad 0.75 < \rho < 0.825\,(\mathrm{Mg\,m^{-3}})$$
$$V_b = 0.7234\,(1/\rho - 1/\rho_i), \quad 0.825 < \rho.$$

There is a regional difference for the profile of V_b for each site; V_b in ice cores from warmer sites is slightly higher than those for ice cores from colder sites in a density range 0.76–0.81 ($\mathrm{Mg\,m^{-3}}$). Peak bubble volumes at which the above two lines are crossed (V_{cb}) are selected as a reference parameter. The 10% value of V_{cb} (V_{ib}) is also selected as another reference parameter. It was found that ρ_{ib} (corresponding density of V_{ib}) ranges from 0.763 to 0.791 $\mathrm{Mg\,m^{-3}}$ and ρ_{cb} (corresponding density of V_{cb}) ranges from 0.819 to 0.832 $\mathrm{Mg\,m^{-3}}$. ρ_{ib} seems to be correlated with ice temperature in ice sheets ($r = 0.81$). The corresponding porosity of ρ_{cb} does not seem to be correlated with ice temperature or accumulation rate. P_{cb} (overburden pressure for ρ_{cb}) ranges from 0.29 to 0.52 MPa and P_{ib} (overburden pressure for ρ_{ib}) ranges from 0.25 to 0.46 MPa. A correlation between P_{ib} and ice temperature ($r = 0.93$) and also between P_{cb} and ice temperature ($r = 0.92$) is observed.

For further studies on the firn–ice transition, the ice-deformation behavior should be considered as explaining the bubble formation and compression processes separately. In particular, the bubble-compression process in the firn–ice transition layer must be clarified quantitatively to understand the regional difference in the total air content in glacier ice and also for understanding the densification behavior of glacier ice after pore close-off.

ACKNOWLEDGEMENTS

We should like to thank Professor S. Mae and Dr M. Nakawo for useful suggestions prior to this study. We also acknowledge Professor E. Akitaya for support during the development of a measuring system for air-bubble volume in ILTS, Hokkaido University. Fruitful discussions with Professors H. Shoji and S. Takahashi are acknowledged. Ice cores from Antarctica were recovered by the 21st, 24th, 25th and 26th Japanese Antarctic Research Expeditions in the Glaciological Research Program in east Dronning Maud Land. The recovery of the site J ice core was supported by a grant-in-aid from the International Scientific Research Program of the Japanese Ministry of Education, Science and Culture.

REFERENCES

Bader, H. 1964. Density of ice as a function of temperature and stress. *CRREL Spec. Rep.* 64.

Fujii, Y. 1978. Miscellaneous compiled data. VI. Temperature profile in the drilled hole. *Mem. Natl Inst. Polar Res. Spec. Issue*, 10, 169.

Higashi, A., *ed.* 1988. *Lattice defects in ice crystals.* Sapporo, Japan, Hokkaido University Press.

Kameda, T., H. Shoji, K. Kawada, O. Watanabe and H.B. Clausen. 1994. An empirical relation between overburden pressure and firn density. *Ann. Glaciol.*, **20** (see paper in this volume).

Langway, C.C., Jr, H. Shoji, A. Mitani and H.B. Clausen. 1993. Transformation process observations of polar firn to ice. *Ann. Glaciol.*, **18**, 199–202.

Maeno, N., H. Narita and K. Araoka. 1978. Measurements of air permeability and elastic modulus of snow and firn drilled at Mizuho Station, East Antarctica. *Mem. Natl Inst. Polar Res. Spec. Issue.*, 10, 62–76.

Martinerie, P., D. Raynaud, D.M. Etheridge, J.-M. Barnola and D. Mazaudier. 1992. Physical and climatic parameters which influence the air content in polar ice. *Earth Planet. Sci. Lett.*, **112**, 1–13.

Moore, J.C., H. Narita and N. Maeno. 1991. A continuous 770-year record of volcanic activity from East Antarctica. *J. Geophys. Res.*, **96**(D9), 17,353–17,359.

Nakawo, M., H. Ohmae, F. Nishio and T. Kameda. 1989. Dating the Mizuho 700-m core from core ice fabric data. *Proceedings of the National Institute of Polar Research (Tokyo) Symposium on Polar Meteorology and Glaciology, 2,* 105–110.

Satake, H., K. Kawada, K. Tsushima and N. Sato. 1986. Isotope study of depositional environment in east Queen Maud Land, Antarctica. *Tritium Research Center Report* (Toyama University)., 6, 57–69 (In Japanese with English abstract.)

Schwander, J. and B. Stauffer. 1984. Age difference between polar ice and the air trapped in its bubbles. *Nature*, **311**(5981), 45–47.

Schwander, J. *and 6 others.* 1993. The age of the air in the firn and the ice at Summit, Greenland. *J. Geophys. Res.*, **98**(D2), 2831–2838.

Shoji, H., H.B. Clausen and T. Kameda. 1991. Accumulation rate at Site J and Dye 2, Greenland. *Bull. Glacier Res.*, **9**, 85–88.

Stauffer, B., J. Schwander and H. Oeschger. 1985. Enclosure of air during metamorphosis of dry firn to ice. *Ann. Glaciol.*, **6**, 108–112.

Suzuki, Y. and K. Shiraishi. 1982. The drill system used by the 21st Japanese Antarctic Research Expedition and its later improvement. *Mem. Natl Inst. Polar Res. Spec. Issue*, 24, 259–273.

Takahashi, S., Y. Ageta, Y. Fujii and O. Watanabe. 1994. Surface mass balance on east Dronning Maud Land in Antarctica observed by Japanese Antarctic Research Expeditions. *Ann. Glaciol.*, **20** (see paper in this volume).

The accuracy of the references in the text and in this list is the responsibility of the authors, to whom queries should be addressed.